Cat-doping: Novel method for phosphorus and boron shallow doping in crystalline silicon at 80 °C

Hideki Matsumura, Taro Hayakawa, Tatsunori Ohta, Yuki Nakashima, Motoharu Miyamoto, Trinh Cham Thi, Koichi Koyama, and Keisuke Ohdaira
Japan Advanced Institute of Science and Technology (JAIST), Asahidai, Nomi-shi, Ishikawa-ken 923-1292, Japan

(Received 7 August 2014; accepted 2 September 2014; published online 16 September 2014)

Phosphorus (P) or boron (B) atoms can be doped at temperatures as low as 80 to 350 °C, when crystalline silicon (c-Si) is exposed only for a few minutes to species generated by catalytic cracking reaction of phosphine (PH_3) or diborane (B_2H_6) with heated tungsten (W) catalyzer. This paper is to investigate systematically this novel doping method, "Cat-doping", in detail. The electrical properties of P or B doped layers are studied by the Van der Pauw method based on the Hall effects measurement. The profiles of P or B atoms in c-Si are observed by secondary ion mass spectrometry mainly from back side of samples to eliminate knock-on effects. It is confirmed that the surface of p-type c-Si is converted to n-type by P Cat-doping at 80 °C, and similarly, that of n-type c-Si is to p-type by B Cat-doping. The doping depth is as shallow as 5 nm or less and the electrically activated doping concentration is 10^{18} to 10^{19} cm^{-3} for both P and B doping. It is also found that the surface potential of c-Si is controlled by the shallow Cat-doping and that the surface recombination velocity of minority carriers in c-Si can be enormously lowered by this potential control.
 [http://dx.doi.org/10.1063/1.4895635]

I. INTRODUCTION

Impurity doping to crystalline silicon (c-Si) at low temperatures is required for fabrication of various devices such as ultra-large scale integrated circuits (ULSI), thin film transistors for displays, and solar cells. Shallow doping of impurities is also required in fabricating ULSI and other devices, apart from the control of surface potential of c-Si solar cells.

We have discovered that phosphorus (P) atoms can be doped into c-Si at substrate temperatures lower than 350 °C and that the surface of p-type c-Si is converted to n-type by P doping[1,2] when c-Si surface is exposed to the ambient of species generated by catalytic cracking reaction of phosphine (PH_3) gas with heated tungsten (W) catalyzer. Then, we have attempted to dope boron (B) atoms into c-Si similarly by using diborane (B_2H_6) instead of PH_3. However, the detailed story about this novel low temperature doping method, named "Cat-doping", has not been clearly mentioned. This paper is to demonstrate systematically the results of investigation on Cat-doping in detail.

After confirming that metal contamination originating from heated W catalyzer is negligible, the electrical properties of P or B doped layers are studied by the Van der Pauw method based on the Hall effects measurement. The profiles of P or B atoms in c-Si are observed by secondary ion mass spectrometry (SIMS), mainly from back side of samples to eliminate influence of knock-on effects of probing ions. The P profiles after doping through thin oxide layers on c-Si are also observed to confirm the doping depth. It is found that the surface of p-type c-Si is converted to n-type by P Cat-doping at 80 °C, and similarly, that of n-type c-Si is to p-type by B Cat-doping. The doping depth is as shallow as 5 nm or less and the doped carrier concentration is 10^{18} to 10^{19} cm^{-3} for both P and B doping. In addition, as possible application of this novel technology, the control of c-Si surface potential is attempted by the shallow Cat-doping, and it is found that the surface recombination velocity of minority carriers in c-Si is enormously lowered by this potential control.

II. FUNDAMENTALS FOR EXPERIMENTS

A. Apparatus and process parameters

The Cat-doping experiments were carried out by using the conventional apparatus for catalytic chemical vapor deposition (Cat-CVD), often called Hot-Wire CVD. A schematic view of the typical Cat-doping apparatus is shown in Fig. 1. A stainless steel chamber with a diameter of 30 cm and a height of 30 cm was used as the apparatus and tungsten (W) wires with a diameter of 0.5 mm and a length of about 2 m were used as catalyzers. Experimental parameters of Cat-doping are summarized in Table I. In the table, the temperature of catalyzer, the surface area of the catalyzing wire, the substrate temperature, the gas pressure during Cat-doping process, the flow rate of gas X and the distance between the catalyzer and the substrates are referred to as T_{cat}, S_{cat}, T_s, P_g, FR(X) and D_{cs}, respectively. Both PH_3 and B_2H_6 gases

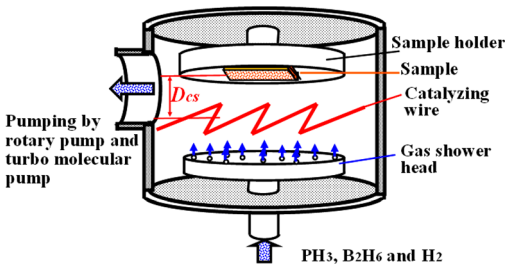

FIG. 1. Schematic view of Cat-doping apparatus.

TABLE I. Parameters for Cat-doping of P and B atoms into c-Si.

	P Cat-doping	B Cat-doping
Temperature of catalyzer, T_{cat}	RT-1800 °C mainly 1300 °C	RT-1800 °C mainly < 1300 °C
Surface area of catalyzer, S_{cat}	31 cm^2	31 cm^2
Temperature of substrate, T_s	RT–350 °C	RT–350 °C
Gas pressure during process, P_g	0.5–3 Pa	0.5–3 Pa
Flow rate of PH_3, FR(PH_3) PH_3 is diluted to 2.25% by helium	0–0.6 sccm	—
Flow rate of B_2H_6, FR(B_2H_6) $B2H_6$ is diluted to 2.25% by helium	—	0–4 sccm
Flow rate of H_2, FR(H_2) Sometimes H_2 is added to doping gas	0–20 sccm	0–20 sccm
Distance between catalyzer and substrate, D_{cs}	12 cm	12 cm
Process time	0.5–240 min	0.5–240 min

were diluted to 2.25% by helium gas, however, here, the flow rate of doping gas is expressed by net values.

For both Cat-CVD and Cat-doping, T_{cat} is one of the most important parameters. However, contrary to CVD, to suppress the surface etching due to hydrogen (H) atoms, produced at catalyzer from H_2 gas or hydrogenated doping gas such as PH_3 or B_2H_6, T_{cat} for Cat-doping is lowered from about 1800 °C of Cat-CVD to about 1300 °C as mentioned below. In addition, the surface contamination of impurities originating from the catalyzer should be carefully avoided. Thus, at first, the effect of surface etching on T_{cat} was investigated, and then, the contamination from the catalyzer was studied.

B. Surface roughness due to etching during process

Figure 2 shows the surface roughness of c-Si as a function of T_{cat}, after exposure to H atoms generated from H_2 at W catalyzer. P_g, FR(H_2), and the process times were 1 Pa, 20 sccm and 60 s, respectively. The surface roughness was measured on an atomic force microscope (AFM) of Digital Instruments NanoScope, IIIa, and the roughness itself is expressed by root mean square (RMS) of measured values. The surface roughness is likely to increase as T_{cat} increases. However, it is only 0.2–0.3 nm for T_{cat} of 1300 °C, although the RMS of original c-Si surface is also around 0.2 nm. From the figure, it is known that the surface roughness is negligible up to T_{cat} of 1300 °C. Thus, in Cat-doping, T_{cat} is mainly fixed at 1300 °C for P Cat-doping and kept at lower than 1300 °C for B Cat-doping, except for experiments of other purposes.

C. Surface contamination during process

Next, the surface contamination was studied by the total reflection X-ray fluorescence (TXRF), using Rigaku, TXRF3750S and the Rutherford back-scattering (RBS), using an accelerator of Nisshin-Highvoltage, NISSHIN-1700 H. Since direct observation of contaminants on surface of c-Si is not easy, the contamination inside a-Si and silicon nitride (SiNx) films both deposited by Cat-CVD was observed to know flux density of contaminants emitted from heated catalyzers. Figure 3 demonstrates the W concentration in deposited a-Si films as a function of T_{cat}. In the figure, apart from our data taken by TXRF and RBS, SIMS data reported by other two groups[3,4] are plotted together. In RBS, 2.0 MeV helium ions were used as incident probing ions.

The W concentration in a-Si is likely to increase as T_{cat} increases. In this case, the deposition rate (DR) of various

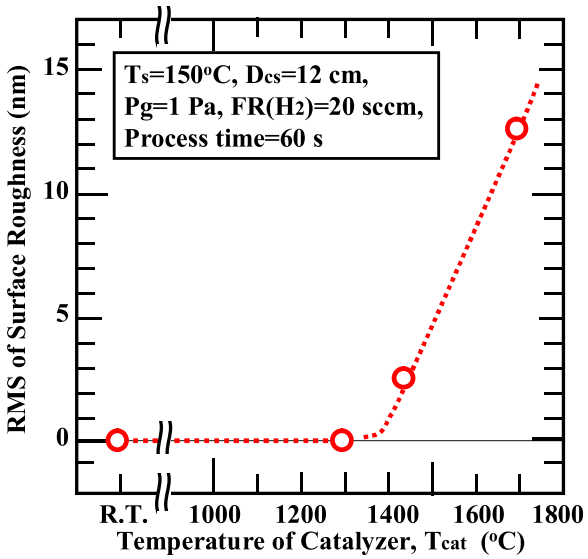

FIG. 2. Surface RMS roughness of c-Si by H etching vs. T_{cat}.

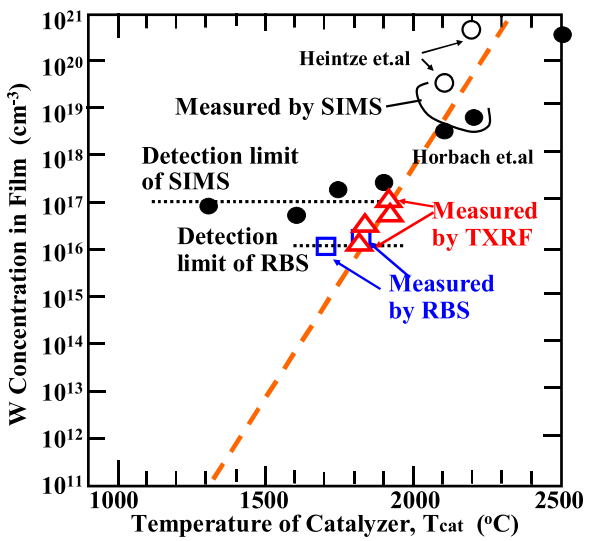

FIG. 3. W concentration in a-Si films vs. T_{cat}.

a-Si films is 0.5–4.0 nm/s and $T_s = 150$–$400\,^{\circ}C$. The deposition conditions for each a-Si film are not same, however, they are in a certain range, that is, P_g, FR(SiH_4) and D_{cs} were 1–5 Pa, 3.6 sccm, and about 1–5 cm, respectively.

Figure 4 demonstrates the sheet density of all impurities which can be detected by TXRF for SiNx films prepared at T_{cat} of 1800 °C by 40 runs of deposition with same deposition conditions.[5] In this case, S_{cat}, FR(SiH_4), FR(ammonia, NH_3), P_g, T_s, and D_{cs} were 88 cm^2, 15 sccm, 300 sccm, 10 Pa, 400 °C and about 4 cm, respectively. DR was about 70 nm/min.

In the films, apart from W, impurities such as iron (Fe), vanadium (V), nickel (Ni), manganese (Mn), zinc (Zn), chromium (Cr), copper (Cu), and titanium (Ti) were detected. Real origin of these contaminants is not clear, however, it is believed that the most of impurities come from W wires as impurities contained in W. In the present experiments, high purity W wires supplied by Allied Materials Corp. were used. The total densities of various impurities are less than $10^{11}\,cm^{-2}$ for $T_{cat} = 1800\,^{\circ}C$. In TXRF, the measured depth is believed to be about 10 nm from penetration depth of X-ray. That is, the atomic density of impurities is roughly estimated to be $10^{17}\,cm^{-3}$ at T_{cat} of 1800 °C. The value is also equivalent to that shown in Fig. 3 for a-Si deposition. Since DR of the film was 70 nm/min, the total number of impurities in a newly grown layer per a minute was estimated to be $7 \times 10^{11}\,cm^{-2}$. This means that the flux density of sum of all impurities emitted from the catalyzer is $7 \times 10^{11}\,cm^{-2}min^{-1}$ for T_{cat} of 1800 °C, D_{cs} of 4 cm, and S_{cat} of 88 cm^2. The value of S_{cat} is larger and D_{cs} is shorter than the present conditions for Cat-doping, and thus, the data appear to make the contamination more serious than the present Cat-doping.

From Fig. 3, it is found that the contamination is lowered by about 5 orders of magnitudes when T_{cat} is lowered from 1800 °C to 1300 °C. That is, the flux density of contaminants is around $7 \times 10^6\ cm^{-2}min^{-1}$ at maximum. As mentioned later, it is found that the sheet carrier density of doping impurities such as P and B atoms is on the order of $10^{12}\,cm^{-2}$ for process time of 60 s. This means that the influence from contamination of any impurities is negligible for Cat-doping when T_{cat} is kept at around 1300 °C.

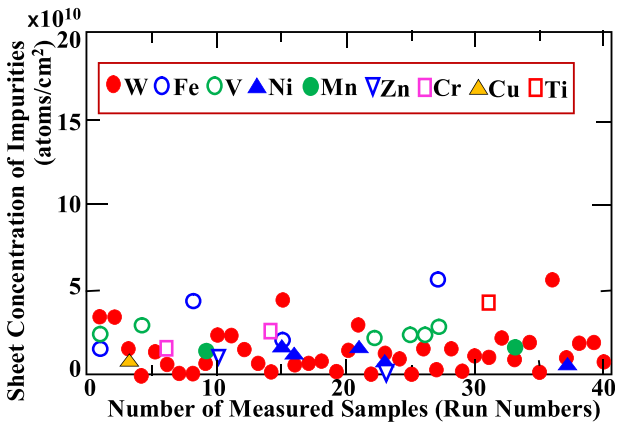

FIG. 4. Sheet concentration of contaminants in Cat-CVD SiNx films.

D. Measurement of electrical properties for Cat-doped samples

The electrical properties of Cat-doped c-Si were measured by the Van der Pauw method, based on the Hall effects measurement. The size of rectangular samples was usually 10 mm × 10 mm, and four electrodes with a diameter of 1 mm were formed at the four corners of rectangular samples. In the Van der Pauw method, the size of electrodes is required as small as possible. However, the present configuration appears enough to obtain the data within error of 10%, according to the model measurements using a simple c-Si sample. The measurement was carried out by using the Hall effects measuring system, Bio-Rad, HL5500PC, mainly at room temperature, but, in some cases, to know the activation energy, it was carried out in various temperatures from 200 K to 310 K.

When the doping depth is shallow, the carrier concentration has a possibility to be influenced by surface defects of c-Si samples. If surface potential of c-Si is forced to be bent because of the surface defects, the measurements of doped carrier density may be affected. Therefore, here, Cat-doped c-Si samples were coated with an intrinsic (i-) amorphous-silicon (a-Si) film, since the interface between a-Si and c-Si is known as almost perfect[6] and a-Si films are often used as passivation films for c-Si surface.[7] In addition, electric conduction through a-Si is possible, although good conduction will not be expected if insulating films such as silicon-dioxide (SiO_2) are used as passivation instead of a-Si.

Figure 5 shows two types of electrodes used in the experiments. One is n-type-a-Si/aluminum (Al) stacked electrodes A, Fig. 5(a), and the other only Al but on thin i-a-Si layer, electrodes B, Fig. 5(b).

Figure 6 shows the sheet carrier density and the carrier mobility of P Cat-doped samples, as a function of the thickness of coated a-Si films. The Cat-doped samples were prepared with $T_s = 150\,^{\circ}C$, $P_g = 1$ Pa, FR(PH_3) = 0.43 sccm and process time of 10 min. The sheet carrier density of the sample without a-Si coating film could be measured only by the stacked electrodes A. The figure shows that coating by a-Si makes measured data stable at about 3–$5 \times 10^{12}\,cm^{-2}$ for case of both electrodes A and B, although the value, $10^{10}\,cm^{-2}$, obtained without i-a-Si coating appears ambiguous due to the effect of surface defects. The mobility of doped layer is about 200 to 300 cm^2/Vs, and the value

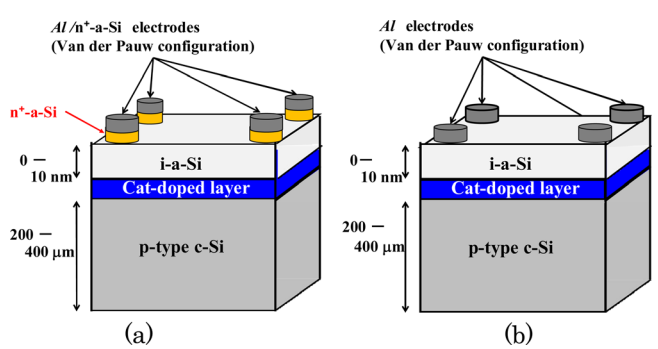

FIG. 5. Structure of electrodes for Van der Pauw measurements: (a) i-a-Si (0-10 nm)/n^+-a-Si/metal and (b) i-a-Si(0-10 nm)/metal.

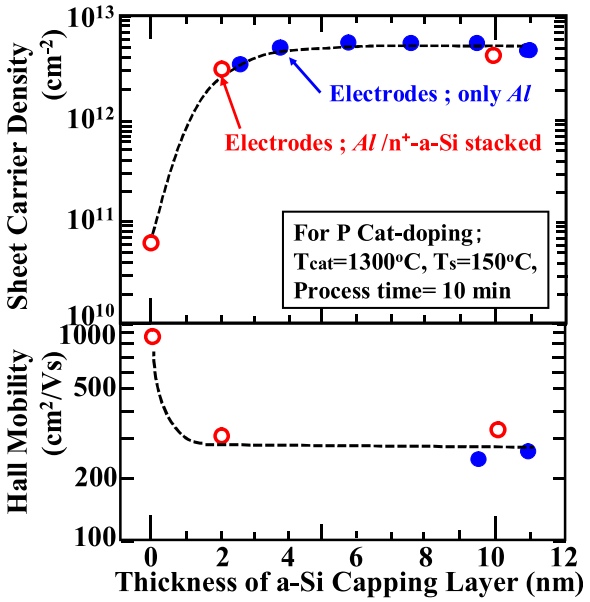

FIG. 6. Sheet carrier density and Hall mobility as a function of thickness of inserted i-a-Si layers for P Cat-doping.

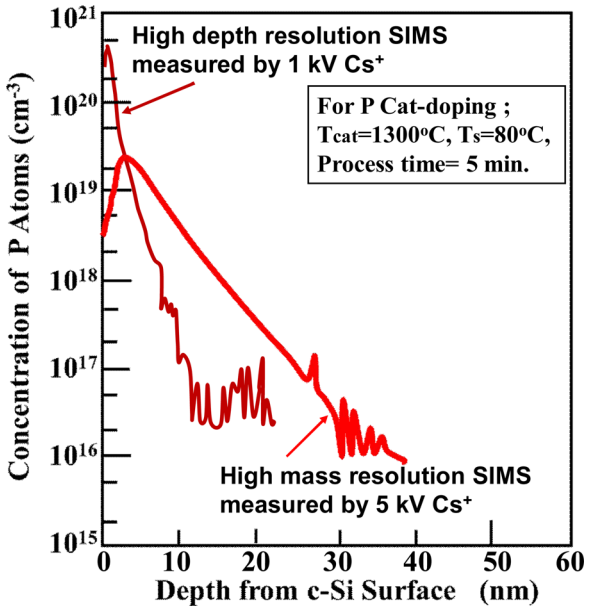

FIG. 7. Concentration of P atoms vs. depth, observed by two types of SIMS systems for high depth resolution and high mass resolution.

appears reasonable for P doped c-Si. That is, the influence of i-a-Si itself does not affect measured data of sheet carrier density. From the figure, here, the electrical properties of Cat-doped samples were evaluated after coating c-Si surface with an about 10 nm-thick i-a-Si layer and evaporating Al with a diameter of 1 mm on them.

E. Measurement of profiles by SIMS

As demonstrated below, Cat-doped P atoms distribute at the depth of about several nm. For observation of such shallow doped impurities, some methods of surface analysis such as X-ray photo-emission spectroscopy (XPS) and Auger electron spectrometry would be considered. However, as also demonstrated below, the concentration of P atoms is usually less than 1 atomic %, that is, less than detection limit of ordinary designed measuring equipment. Thus, here, we chose SIMS to know profiles of doped atoms, although the precise measurements of P profiles by SIMS are not so easy when the doping depth is as shallow as several nm.

For instance, the measurement of P atoms with a mass number of 31, ^{31}P, is likely to suffer from the interference of fragments with the same mass number, formed by the combination of Si isotope of a mass number 30, ^{30}Si, with H atom of a mass number of 1, ^{1}H. Here, for distinguishing the mass difference between ^{31}P and ^{30}Si+^{1}H, we used a high mass resolution SIMS system with a magnetic mass-analyzer using 5 kV primary ions of cesium (Cs), CAMECA, IMS-7F. However, since the relatively high energy is used as primary ions to increase mass resolution, the depth resolution is sacrificed for it. Thus, for the measurements with high depth resolution, we used a different SIMS system, PHI, ADEPT 1010, using a quadrupole mass analyzer with probe ions of 1 keV.

Figure 7 shows the P profiles observed by both IMS-7F and ADEPT 1010, to know the difference of these two systems. P Cat-doping was carried out with $T_s = 80\,^{\circ}C$, $P_g = 1$ Pa, $FR(PH_3) = 0.43$ sccm and process time of 5 min, and the Cat-doped c-Si was coated with a 60 nm-thick i-a-Si prepared by Cat-CVD with $T_{cat} = 1750\,^{\circ}C$, $T_s = 90\,^{\circ}C$, $P_g = 0.5$ Pa and $FR(SiH_4) = 10$ sccm. From the figure, it is known that the depth profiles of P atoms measured by two systems show the different penetration depth and that the penetration depth by the high mass resolution SIMS looks more than 2 times deeper than that by the high depth resolution SIMS. Contrary to it, the peak density of P atoms at interface between c-Si and coated a-Si for the high mass resolution system is about 1/10 smaller than that for the high depth resolution system.

In addition, SIMS has another problem originated from the knock-on effect by probing ions. Figure 8 shows the SIMS profiles of P atoms for the Cat-doped sample prepared with $T_s = 80\,^{\circ}C$ and process time of 60 s. In the figure, two profiles are shown. One is conventional and measured from

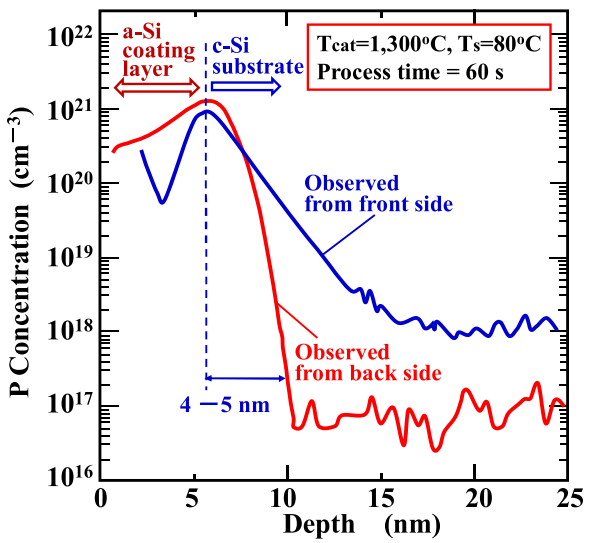

FIG. 8. P Concentration vs. depth, observed by high depth resolution SIMS from both front side and back side of samples.

the front side of sample. The other is measured from the back side of sample by etching. It is clear that when the profile is observed from the front side, it shows the exponential distribution, but when it is observed by the back side, the measured profile looks different. It appears to follow complementary error function (*erfc*) or *Gauss* distributions. Thus, here, we discussed the profiles mainly by using the SIMS data measured from the back side of samples, although the data taken from the front side were often used to know the number of total doped atoms.

III. RESULTS OF CAT-DOPING

A. Electrical properties

At first, the conduction type of Cat-doped samples was checked by the Hall effects measurement. The Hall voltage of the samples were measured under the magnetic flux of 0.32 T, applied normally to the sample surface. Figure 9 demonstrates the Hall voltages as a function of applied currents for both P and B Cat-doped samples. P Cat-doping was carried out to B-doped p-type c-Si with hole concentration of 10^{13} to 10^{14} cm^{-3}, and B Cat-doping was also to P-doped n-type c-Si with electron concentration of 10^{13} to 10^{14} cm^{-3}. In the figure, similar Hall voltage of an original p-type c-Si is demonstrated for comparison. T_s for Cat-doping was 350 °C in this case, however, the results for the sample of $T_s = 80$ °C were not so different from those shown here. From the figure, it is confirmed that the conduction type of P Cat-doped sample is converted to n-type from original p-type, and also that n-type c-Si is converted to p-type by B Cat-doping. This demonstrates that the conduction type can be converted by Cat-doping for T_s much lower than temperatures for the conventional impurity doping by thermal diffusion.

Figure 10 shows the sheet carrier concentration and the conduction types as a function of T_{cat} for P Cat-doping into p-type c-Si mentioned above. In this case, T_s was 80 °C. As

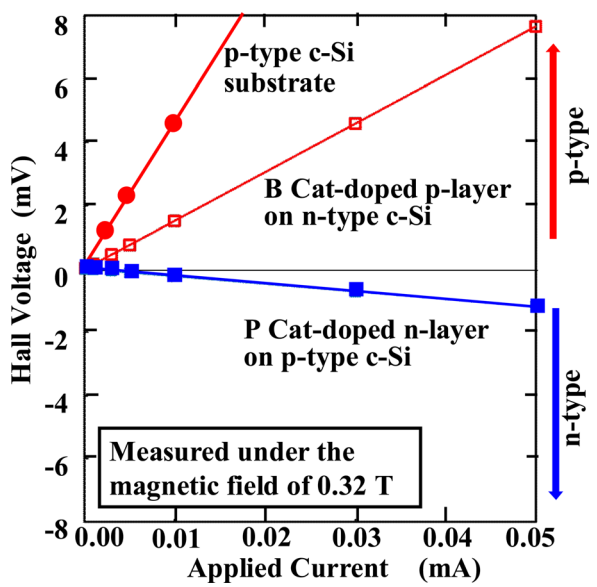

FIG. 9. Hall voltages vs. applied currents for P Cat-doped, B Cat-doped and original p-type c-Si samples.

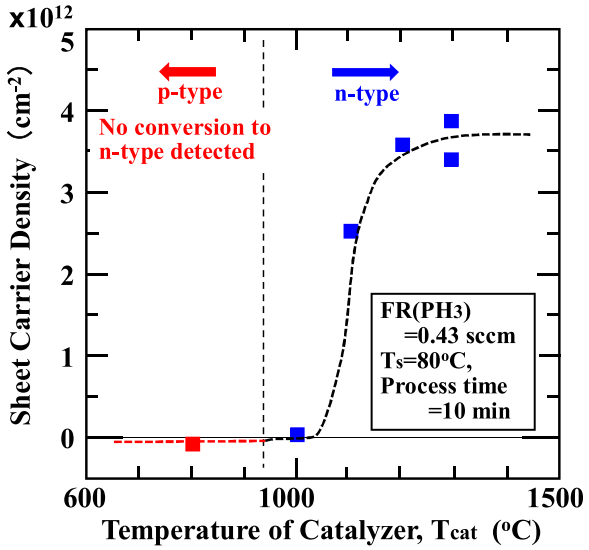

FIG. 10. Sheet carrier density of P Cat-doped c-Si as a function of T_{cat}.

shown in the figure, the sheet carrier density is likely to increase as T_{cat} increases. However, the conduction type is kept p-type for T_{cat} lower than 800 °C, and it is converted to n-type when T_{cat} exceeds 1000 °C. According to the recent reports by Umemoto *et al.*,[8] PH_3 is decomposed to P and H by cracking on W catalyzer heated over 1000 °C, and the amount of such cracked species increases exponentially as T_{cat} increases. This clearly demonstrates that the existence of species generated by cracking of PH_3 is essentially necessary for this low temperature Cat-doping.

As explained below, P atoms distribute at the depth of several nm in c-Si. If doping depth of P atoms is approximated to 5 nm, since the sheet carrier concentration is at the order of 10^{12} cm^{-2} as shown in Fig. 10, the carrier concentration of doped P atoms at near to c-Si surface is estimated to be 10^{18}–10^{19} cm^{-3}. The value appears enough to convert the conduction type.

In case of B Cat-doping, the situation is a little bit complicated. W surface is easily converted to W-boride during process, and this appears to reduce the reproducibility of B Cat-doping. In addition, B_2H_6 is easily thermally decomposed. For instance, when T_s is 350 °C, the surface of n-type Si is converted to p-type by B doping even if the catalyzer is not heated. B_2H_6 is thermally decomposed for T_s over about 300 °C and the simple thermal diffusion appears to occur for B doping at $T_s = 350$ °C. However, when T_s is 80 °C, B doping cannot be detected when the catalyzer is not heated.

Figure 11 demonstrates the sheet carrier density of B Cat-doped samples as a function of T_{cat}, taking T_s as a parameter. B Cat-doping was carried out into n-type c-Si with electron carrier concentration of 10^{13} to 10^{14} cm^{-3} as similar as the case mentioned in Fig. 9. When T_s is kept at 80 °C, the effect of B Cat-doping is clear, and the conduction type is converted from original n-type to p-type as T_{cat} increases at over 500 °C. T_{cat} required for the conversion of conduction type appears different from that for P Cat-doping and much lower than that. In addition, when T_s is 350 °C, the surface of c-Si is already converted to p-type by the simple thermal diffusion in addition to Cat-doping. For T_{cat} over 1000 °C, the

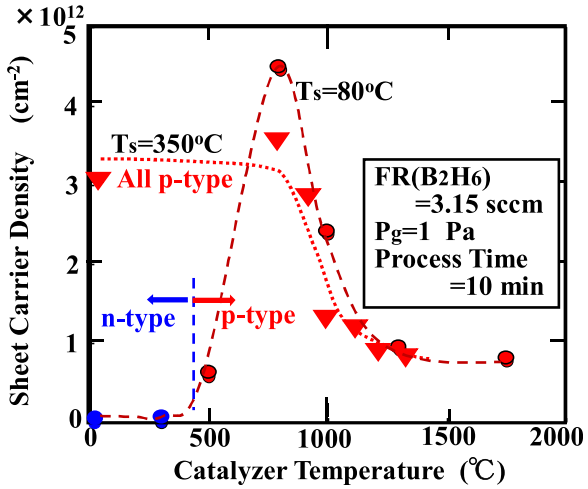

FIG. 11. Sheet carrier density of B Cat-doped c-Si as a function of T_{cat}.

sheet carrier density for the samples at both $T_s = 80\,°C$ and 350 °C is likely to decrease. This may be caused by forming W-boride on W catalyzing wires and losing sufficient species to control the carrier density of c-Si. The reproducibility of B Cat-doping for T_{cat} over 1000 °C appears quite low. The sheet carrier density for T_{cat} over 1000 °C is likely to fluctuate depending on how long the catalyzer is used. For B Cat-doping, T_{cat} lower than 1000 °C appears better.

B. Profiles of Cat-doped atoms

In SIMS measurements, if a real P profile is so sharp, approximately a delta function, the observed profile becomes a *Gauss* distribution (*Gaussion*) due to the depth resolution of measuring system.

Figure 12 demonstrates the plots of P profile which have been already shown in Fig. 8 as a profile observed from the back side of a sample. When the surface of c-Si is exposed to P-related species with constant concentration, doped P profile should be expressed by *erfc* as a solution of the conventional diffusion equation. The profile in the figure appears to follow *erfc*. However, the difference between *erfc* and *Gaussian* is quite small, and the profile appears also to follow *Gaussian* as shown in Fig. 12. This may mean that the P Cat-doped depth is so shallow, several nm or less, and equivalent to the value of depth resolution.

Figure 13 also demonstrates two P profiles for Cat-doped samples with $T_s = 80\,°C$, $P_g = 1\,Pa$, process times of 1 min and 4 min. When the process times increases, the profile appears to spread slightly. However, the difference of two profiles is quite small and sometimes depends on the difference of depth resolution for each measurement. Actually, when the process times increases to 16 min, the profiles are not so different from that of 4 min, although the expansion of distribution is expected depending on the root of times. The time dependence of the profiles will be discussed later.

C. Activation energy of carrier density

From the above results, it is known that the doping depth is limited at a region adjacent to the surface. In that case, how P atoms are incorporated in c-Si structure? To know it, next, we measured the temperature dependence of the sheet carrier density of P Cat-doped sample prepared with $T_s = 80\,°C$, $P_g = 1\,Pa$ and process time of 60 s. Figure 14 shows the sheet carrier density of such a sample as a function of reciprocal of measured temperatures for range from 200 K to 310 K. Since the absolute values of sheet carrier density are likely to fluctuate for sample to sample, it is expressed by arbitrary unit to avoid confusion. The activation energy for this temperature range is believed to show the effect of doping impurity. The value is about 0.045 eV and appears normal for the c-Si in which P atoms are substituted into Si-sites and working as donors. That is, P atoms appear to work as similar as those incorporated into c-Si by high temperature thermal processes.

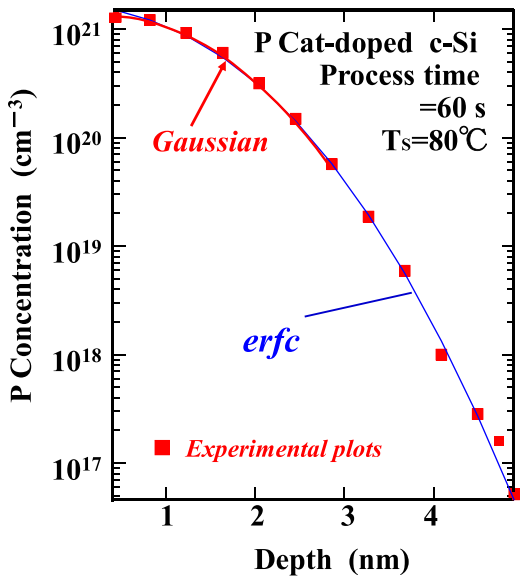

FIG. 12. P concentration vs. depth by SIMS from the back side. Fitting results using *erfc* and *Gaussian* are also shown for comparison.

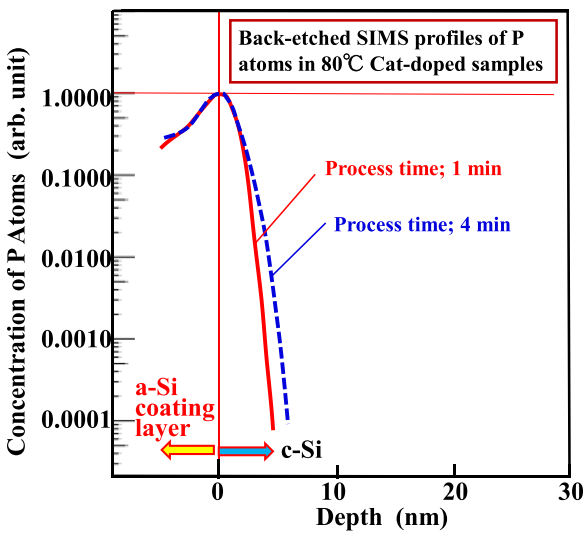

FIG. 13. P concentration vs. depth by SIMS from the back side for Cat-doped samples with process times of 1 and 4 min.

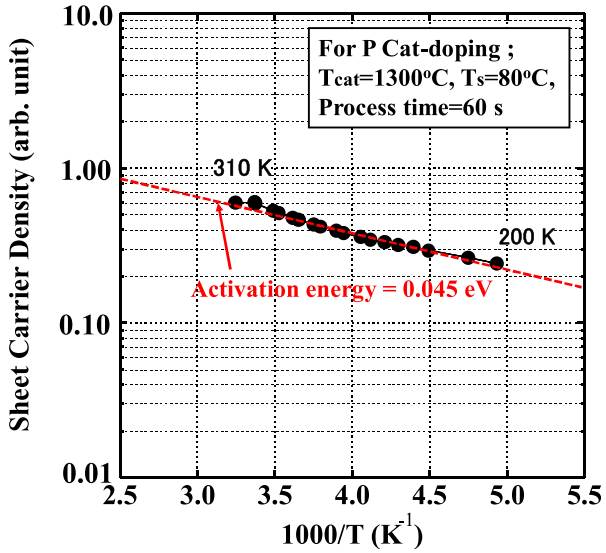

FIG. 14. Sheet carrier density (arbitrary unit) as a function of T_{cat} to derive activation energy.

D. P Cat-doping through thin oxide layer

Since P Cat-doping depth is so shallow and it does not appear easy to know exact doping depth from SIMS data, we attempted to dope P atoms through very thin silicon-oxide (SiOx) layers formed on c-Si surface and to measure the sheet carrier density after removing SiOx layers of various thicknesses. The SiOx layer is prepared by dipping c-Si in boiled hydrogen peroxide (H_2O_2) solution for several minutes at about 90 °C. Since the control of SiOx thickness is not easy, we selected the c-Si samples with various thick SiOx layers. The thickness of SiOx layers is measured on an ellipsometer of Woolam, V-VASE. After P Cat-doping, the SiOx layer is removed by 2% hydro-fluoric acid (HF) solution and after that the surface is immediately covered with a 10 nm-thick Cat-CVD i-a-Si layer for Van der Pauw measurements.

Figure 15 demonstrates the sheet carrier density and the conduction types as a function of the process times, after p-type c-Si samples of the original hole concentration of 10^{13} to $10^{14}\,cm^{-3}$ are Cat-doped by P atoms through SiOx layers with thicknesses of 0 to 7 nm. In the figure, the thickness of SiOx layers is taken as a parameter. P Cat-doping was carried out with $T_s = 350$ °C and $P_g = 1$ Pa. When c-Si is not covered with the SiOx layer, after process time of 1 min, the surface of p-type c-Si is converted to n-type and the sheet carrier density becomes to about 2–3 × $10^{12}\,cm^{-2}$. However, when c-Si is covered with 4 nm-thick SiOx, the surface of p-type c-Si is not converted to n-type at the process time of 1 min but converted after the process times over 5 min. When the thickness of SiOx is 7 nm, no conversion is observed any more. In addition, even after the conduction type is converted, the sheet carrier density cannot reach the value of the sample without SiOx.

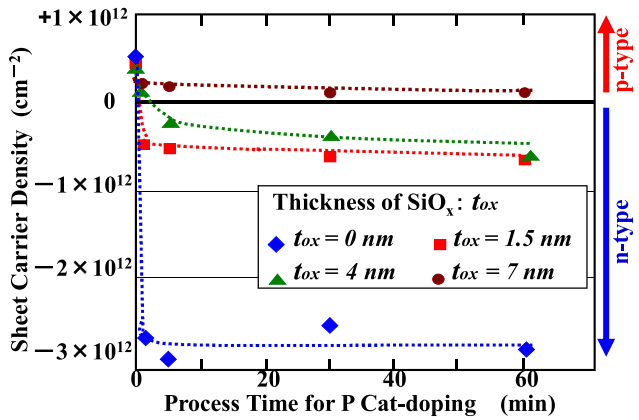

FIG. 15. Sheet carrier density of samples P-Cat-doped through 1.5 nm-thick SiOx, as a function of process times, taking thickness of SiOx as a parameter.

These results clearly demonstrate that Cat-doping phenomena are not caused by simple adsorption of unknown species on c-Si surface, P atoms can diffuse through a thin SiOx layer, and that P atoms reaching to c-Si are working as donors. Although the penetration depth of P atoms inside c-Si is still not known from the present experiment, the results shown in Figs. 12–14 suggest that it is the depth where P atoms are surrounded by many Si atoms in c-Si, but shallower than several nm. However, at the same time, it should be also noted that the sheet carrier density is likely to saturate after the process times over several min. If the phenomena are attributed to a simple diffusion process, the value should increase monotonically as the process time increases. This is discussed later.

IV. DEVICE APPLICATION OF CAT-DOPING

The Cat-doping is a newly developed technology, and the study on the mechanism of low temperature impurity doping is still under the way. However, the feasibility of device application is apparent. The shallow doping can be used to control the surface potential of various semiconductor devices. For instance, the surface passivation for c-Si solar cells can be improved by the electric field effects due to shallow Cat-doping.

The c-Si surface can be passivated with i-a-Si or SiNx layer prepared on it. We have already reported the improvement of passivation quality of Cat-CVD i-a-Si[9] and SiNx[10,11] films by introducing Cat-doping, prior to the deposition of such passivation films. However, to demonstrate the usefulness of Cat-doping and also to confirm P atom doping at low temperatures, we summarize the reported results of passivation by both i-a-Si and SiNx layers.

Figure 16 demonstrates the carrier lifetimes of i-a-Si/c-Si and SiNx/c-Si samples as a function of FR(PH_3) for Cat-doping. The c-Si is n-type with electron density of 10^{13} to $10^{14}\,cm^{-3}$. Cat-doping was carried out at $T_s = 150$ °C, $P_g = 1$ Pa and process time of 60 s for i-a-Si passivation samples[9] and at $T_s = 80$ °C, $P_g = 1$ Pa and process time of 60 s for SiNx passivation samples.[10,11] In Cat-doping for i-a-Si passivation samples, H_2 gas of FR(H_2) = 20 sccm was added to PH_3. The i-a-Si films were deposited at $T_{cat} = 1700$ °C, $P_g = 0.64$ Pa, FR(SiH_4) = 20 sccm, $T_s = 150$ °C and SiNx films at $T_{cat} = 1800$ °C, $P_g = 10$ Pa, FR(SiH_4) = 8 sccm, FR(NH_3) = 150 sccm, $T_s = 100$ °C but after deposition the

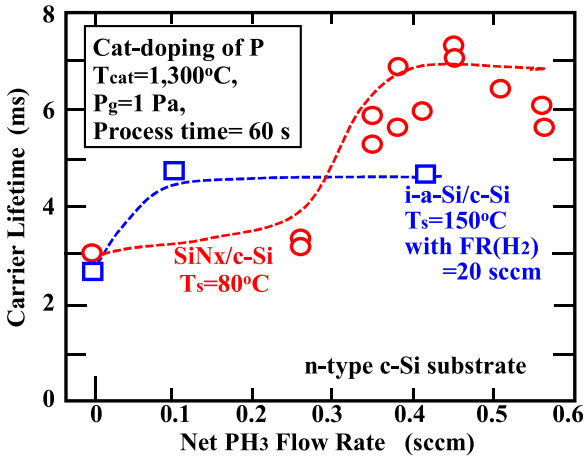

FIG. 16. Carrier life times for i-a-Si and SiNx coated c-Si samples which are both P-Cat-doped prior to deposition of coating film, as a function of $FR(PH_3)$.

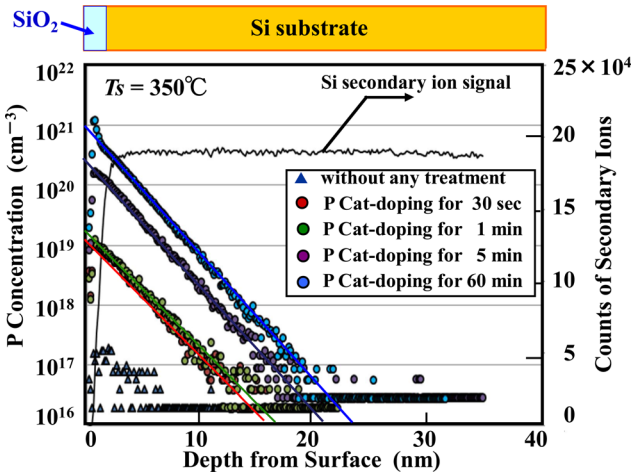

FIG. 17. P concentration vs. depth by SIMS from the front side of samples, after P Cat-doping through 1.5 nm-thick SiOx layer.

SiNx passivation samples were annealed at 350 °C for 30 min.

The carrier lifetime was measured by micro-wave photo-conductivity decay (μ-PCD) method using Kobelco, LTA-1510P. In the method, 10 GHz micro-wave is used to detect the photo-induced carriers in c-Si, and a laser with a wavelength of 904 nm is used to generate photo-carriers in c-Si. It is clear from the figure that the carrier lifetimes can be easily improved by Cat-doping of P atoms prior to deposition of i-a-Si or SiNx. Taking account of the thickness of c-Si wafers, about 280–290 μm, the maximum surface recombination velocity is evaluated under the assumption that all carriers are not recombined in bulk at all but only at the surface. The values are about 3 cm/s for 100 nm-thick i-a-Si passivation samples[9] and 2 cm/s or less for 100 nm-thick SiNx passivation samples.[11]

SiNx layers are widely used as anti-reflection coating for c-Si solar cells. However, it is not so easy to obtain high carrier lifetimes for the direct deposition of SiNx on c-Si with the resistivity of several Ωcm suitable to solar cells. The maximum surface recombination velocity estimated to be 2 cm/s or less is one of the best records for solar-cell-usable c-Si with the resistivity of 1–5 Ω cm for single SiNx passivation.

The results demonstrate the positive effect of Cat-doping. When P atoms with carrier concentration of 10^{18}–10^{19} cm^{-3} are incorporated at near to c-Si surface of original doping concentration of 10^{13}–10^{14} cm^{-3}, the band near to c-Si surface is likely to bend down about 0.2 eV. Holes are repulsed from c-Si surface by this band-bending, and the surface recombination is suppressed. Cat-doping is a new useful tool for controlling surface potential of semiconductors.

V. DISCUSSIONS

A. Features of Cat-doping

It is known from above experiments that (1) P and B atoms are incorporated into c-Si at the temperatures as low as 80 °C, however, that 2) the doping depth is as shallow as 4–5 nm or less. Since the doping depth is almost equivalent to a scale of depth resolution in SIMS analysis, the exact estimation of doping depth appear ambiguous. It is also known that the extension of doping depth appears slow even if the process time is prolonged although P and B atoms can be incorporated in the times as short as 60 s.

Figure 17 shows SIMS P profiles which were measured from the front side of samples in this case. The samples are the same ones whose carrier density is demonstrated in Fig. 15. The c-Si samples coated with 1.5 nm-thick SiOx were used for measurements. Since the profiles were taken from the front side, all profiles were expressed in exponential shapes due to the knock-on effects as mentioned already. The SIMS profiles were taken in high mass resolution system with the probe ions of 5 keV. In the figure, P Cat-doping was carried out at $T_s = 350$ °C, $P_g = 1$ Pa for various process times. Although the correct information on the shape of profiles can not be obtained due to the knock-on effects, the total number of incorporated doping atoms can be evaluated by the integral of profile along depth.

Figure 18 shows the relationship between the total P atoms evaluated by the integral of profiles in Fig. 17 and the

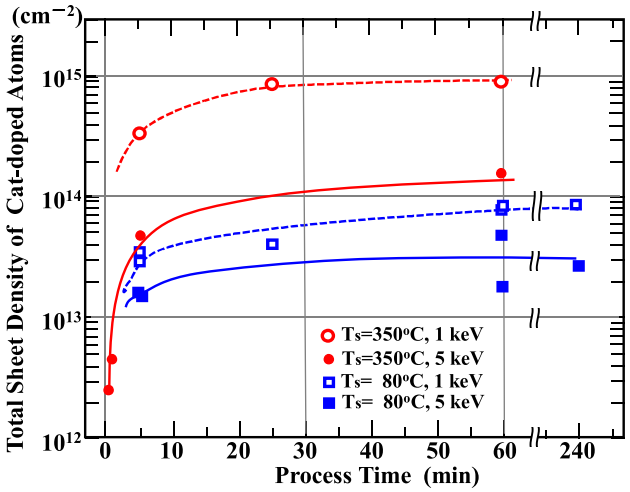

FIG. 18. Total sheet density of Cat-doped P atoms vs. process times.

process times. In the figure, results of some other experiments are demonstrated together. The evaluated values from SIMS profiles, taken by high depth resolution system with the probe ions of 1 keV, are plotted with open circles or open squares. The results by high mass resolution system with the probe ions of 5 keV are also plotted with closed circles or closed squares. The results for both $T_s = 350\,^{\circ}C$ and $80\,^{\circ}C$ are demonstrated. It is known that the total number of P atoms observed in high depth resolution system is always larger than those in high mass resolution system since the effect of $^{30}Si+H$ fragments is included in high depth resolution data. It is also known that total number of incorporated P atoms is likely to saturate as the process time increases. If the phenomena simply follow thermal diffusion, the number of incorporated atoms should be proportional to the root of process times. When the process time is shorter than 25 min, such relation appears to hold. If we estimate the diffusion constant of Cat-doping in such a short process time, it would be by several to 10 orders of magnitudes larger than that of the conventional thermal diffusion. However, even if the process time is prolonged over 25 min, it does not increase any more and the phenomena are not likely to follow simple diffusion theory. We have to consider some new mechanisms for understanding Cat-doping phenomena.

B. Activation ratio of incorporated atoms

From the results shown in Figs. 15 and 18, and also, from Figs. 10 and 18, the activation ratio of doped P atoms can be estimated. Here, the activation ratio is defined as the ratio of electrically activated impurities to the total number of incorporated impurities. Since the sheet carrier density of P Cat-doped c-Si without SiOx coating shown in Fig. 15 and the sheet density of incorporated P atoms shown in Fig. 18 are about $2–3 \times 10^{12}$ cm^{-2} and $0.5–1 \times 10^{14}$ cm^{-2}, respectively, the activation ratio is simply evaluated to be about 2–6% for Cat-doping at $T_s = 350\,^{\circ}C$. Similarly, for Cat-doping at $T_s = 80\,^{\circ}C$, it is evaluated to be 7–10%. We have also observed SIMS profiles and measured the sheet carrier density for some other samples not shown here. The fluctuation appears quite large, the activation ratio distributes from 2% to 10% even for Cat-doping at the same T_s. Thus, at the moment, we do not particularly conclude from the data for the present range of temperatures that the activation ratio is depending on T_s.

C. Mechanism of Cat-doping

As mentioned above, P and B atoms are incorporated into c-Si at temperatures as low as $80\,^{\circ}C$ and with process times as short as 60 s. When the process time is shorter than 25 min, the incorporation of atoms appears to follow the simple diffusion theory, but after that, it is likely to saturate. This may suggest that there is an unknown special region at near to c-Si surface. In the region, foreign atoms can be easily incorporated until their concentration exceeds $10^{20}\,cm^{-3}$, judging from Fig. 18 and assuming the doping depth of 5 nm. We have obtained no direct evidence of the existence of such special region. Therefore, at the moment, the exact mechanism of Cat-doping can not be clearly revealed. However, we have already discovered other phenomena similar to the present Cat-doping.

We have reported on low temperature thermal oxidation of c-S.[12,13] When c-Si is exposed to species generated by catalytic cracking reaction of H_2 diluted oxygen (O_2) gas with heated W catalyzer, the surface of c-Si can be oxidized and converted to SiO_2 even at the temperatures as low as $200\,^{\circ}C$. The SiO_2 appears to have sufficient electrical properties as a gate insulator. At that time, we attempted to increase the oxidized thickness, however, the thickness of SiO_2 appeared to be limited at about 4 nm.[13]

On the other hand, we have also discovered that nitrogen (N) atoms are sometimes incorporated into c-Si during deposition of SiNx using NH_3 and SiH_4 gases, and that such a N incorporated layer forms a defect layer in c-Si to degrade passivation quality for SiNx/c-Si system.[14] Observation by transmission electron microscope (TEM) demonstrates that the depth of such defect layer is again at about a few nm to several nm.[14]

All these experiments including the present Cat-doping demonstrates that foreign atoms can be incorporated into c-Si at low temperatures when it is exposed to species generated by catalytic cracking reactions with heated W catalyzer. Although the mechanism is not clearly explained, it is clear that the phenomena concerned with low-temperature doping surely exist.

D. Effect of hydrogen

Another thing we have to consider is the existence of H atoms at the vicinity of incorporated P atoms. From all experiments, incorporation of atoms into c-Si at low temperatures always requires the cracked species. In all experiments concerned with P and B Cat-doping, low temperature oxidation and N incorporation, high density H atoms are also generated during the experimental process. Figure 19 shows the SIMS profiles of P atoms and H atoms for Cat-doping at $T_s = 80\,^{\circ}C$, Fig. 19(a), and $T_s = 350\,^{\circ}C$, Fig. 19(b). c-Si samples were coated with i-a-Si layers. The profiles were taken from the back side of the samples by high depth resolution system with the probe ion energy of 1 keV. In this measurement, since the isotope fragments of $^{30}Si+H$ are included, P profile itself is strongly affected by H profile.

However, the shape of P profiles is not always same to that of H profiles, particularly in the region of coated a-Si layer. This suggests that P profile itself is believable although the P profile suffers from the isotope fragments and, thus, the absolute value of density is not correct. The figure demonstrates that P atoms distribute at the same region where H atoms distribute. The H profiles are almost overlapped with P profiles. This suggests that low temperature Cat-doping of P atoms might be affected by the existence of H atoms.

According to our *ab initio* calculation for a model of c-Si system consisting of 216 Si atoms and an additional single P atom and a single H atom in them, the P atom has energetically stable 4 possible configurations corresponding to 4 sites in c-Si lattice when the H atom exists just adjacent to the P atom. And such a P atom can hop to another site of 0.1–0.2 nm far from the initial site with activation energy of about 0.8 eV or less. When the P atoms move into c-Si by

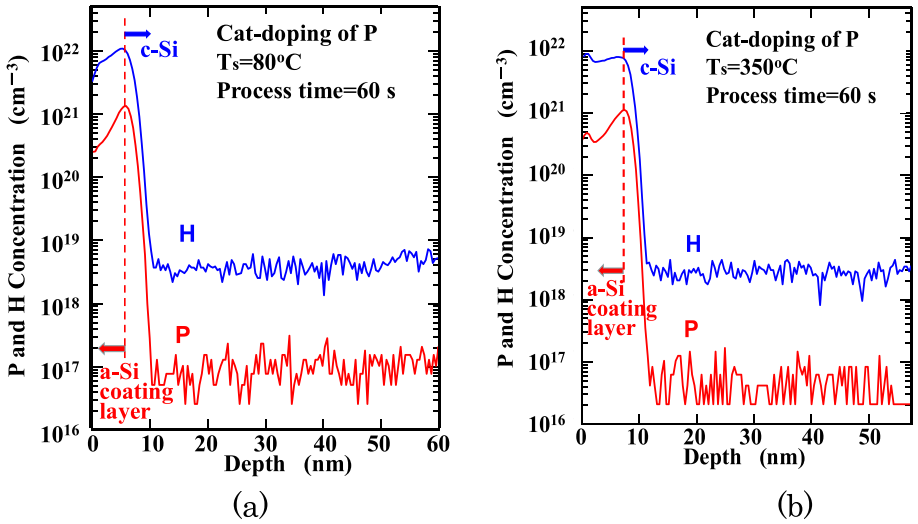

FIG. 19. SIMS profiles of P and H atoms, observed from the back side, for P-Cat-doped samples at (a) $T_s = 80\,^{\circ}C$, and (b) $350\,^{\circ}C$.

substitutional diffusion, the activation energy is about 3.0 eV. The *ab initio* calculation suggests that P atoms can diffuse easily when H atoms exist in c-Si. This again suggests that there may be a help of H atoms in low temperature P diffusion or low temperature incorporation of foreign atoms into c-Si. The result of *ab initio* calculation will be reported in detail elsewhere.[15]

The unknown region existing at near to c-Si surface, speculated above, may be also concerned with incorporation of H atoms. That is, there may be a special region where H atoms can be easily incorporated and other foreign atoms can be incorporated by following such H atoms. However, at the moment, everything is only under speculation. Further efforts to reveal mechanism of Cat-doping are required, although the phenomena are clearly revealed and the feasibility of application are demonstrated in the present paper.

VI. CONCLUSIONS

As mentioned above, Cat-doping is studied in detail in the present paper. There are some unknown matters including the mechanism. However, so far, the following conclusions are obtained.

(1) When c-Si is exposed to species generated by the catalytic cracking reaction of PH_3 or B_2H_6 gas with heated W catalyzer, P or B atoms are doped in c-Si at the temperatures as low as $80\,^{\circ}C$. This novel doping method is called "Cat-doping".
(2) By Cat-doping of P atoms, p-type c-Si is converted to n-type, and similarly by Cat-doping of B atoms, n-type c-Si is converted to p-type, even at the substrate temperatures as low as $80\,^{\circ}C$.
(3) Cat-doped layer is formed at the depth as shallow as 5 nm or less.
(4) By using Cat-doping technology, the surface potential of c-Si can be easily controlled, and through this control, the surface recombination velocity of carriers in c-Si can be enormously lowered for both i-a-Si and SiNx passivation on c-Si. Further device application is expected.

ACKNOWLEDGMENTS

This work was supported by CREST Research Program of Japan Science and Technology Agency of Government (JST). The authors are grateful to advisory committee members of the CREST for their discussions and to students of Japan Advanced Institute of Science and Technology (JAIST) for their experimental supports. The authors are also grateful to Mr. S. Osono and his co-workers at ULVAC Corporation for providing TXRF data.

[1]T. Hayakawa, Y. Nakashima, M. Miyamoto, K. Koyama, K. Ohdaira, and H. Matsumura, Jpn. Appl. Phys., Part 1 **50**, 121301 (2011).
[2]T. Hayakawa, Y. Nakashima, K. Koyama, K. Ohdaira, and H. Matsumura, Jpn. J. Appl. Phys., Part 1 **51**, 061301 (2012).
[3]M. Heintze, R. Zedliz, H. N. Wanka, and M. B. Schubert, J. Appl. Phys. **79**, 2699 (1996).
[4]C. Horbach, W. Beyer, and H. Wagner, J. Non-Cryst. Solids **137–138**, 661 (1991).
[5]S. Osono, Y. Uchiyama, M. Kitazoe, K. Saitoh, M. Hayama, A. Masuda, A. Izumi, and H. Matsumura, Technical Digest of 2002 Fall Meeting of Japan Society of Applied Physics (JSAP), Niigata, Japan, Sept., 2002, (JSAP, 2002), 26a-C-5, p.732.
[6]K. Koyama, K. Ohdaira, and H. Matsumura, Appl. Phys. Lett. **97**, 082108 (2010).
[7]G. Citarella, M. Grimm, S. Schmidbauer, K. H. Ahn, M. Erdmann, T. Shulze, M. Plettig, B. Gruber, J. Hausmann, R. Bohme, W. Stein, D. Muller, M. Winkler, T. Zerres, E. Vetter, D. Batzner, B. Strhm, D. Lachenal, G. Wahli, F. Wunsch, P. Papet, Y. Andrault, C. Guerin, A. Buchel, and B. Rau, *Proceedings of the 26th EU Photovoltaic Specialists Conference, Hamburg, Germany, 2011* (IEEE, 2011), p. 865.
[8]H. Umemoto, Y. Nishihara, T. Ishikawa, and S. Yamamoto, Jpn. J. Appl. Phys., Part 2 **51**, 086501 (2012).
[9]H. Matsumura, M. Miyamto, K. Koyama, and K. Ohdaira, Sol. Energy Mater. Sol. Cells **95**, 797 (2011).
[10]T. C. Thi, K. Koyama, K. Ohdaira, and H. Matsumura, Tech. Dig. - Photovoltaic Sci. Eng. Conf. **2013**, 1-O-24.
[11]T. C. Thi, K. Koyama, K. Ohdaira, and H. Matsumura, J. Appl. Phys. **116**, 044510 (2014).
[12]A. Izumi, S. Sohara, M. Kudo, and H. Matsumura, Electrochem. Solid-State Lett. **2**, 388 (1999).
[13]A. Izumi, Thin Solid Films **395**, 260 (2001).
[14]K. Higashimine, K. Koyama, K. Ohdaira, H. Matsumura, and N. Otsuka, J. Vac. Sci. Technol. B **30**, 031208 (2012).
[15]D. H. Chi, (private communication).